Draft version May 24, 2019
Preprint typeset using LaTeX style emulateapj v. 6/22/04



# RULING THE UNIVERSE: AN IMPROVED METHOD FOR MEASURING $H_0$ WITH GALAXY CLUSTERS

Eric J. Hallman and Jack O. Burns
Center for Astrophysics and Space Astronomy, University of Colorado, Boulder, CO 80309

Patrick M. Motl
Department of Physics and Astronomy, Louisiana State University, Baton Rouge, LA 70803

Michael L. Norman
Center for Astrophysics and Space Sciences, University of California-San Diego, 9500 Gilman Drive, La Jolla, CA 92093
*Draft version May 24, 2019*

## ABSTRACT

We present a new method of calculating the value of the Hubble constant ($H_0$) from combined X-ray/SZE observations of clusters of galaxies. Values of $H_0$ reported from cluster observations are systematically low compared to other methods. We show using a large sample of numerically simulated clusters at a variety of redshifts that the typically used method of calculating $H_0$, which assumes the cluster gas to be isothermal, results in a 20-30% underestimate of the value of $H_0$. The new method, which assumes the cluster gas temperature has a radial dependence described by a universal temperature profile, results in a value much closer to the true value of $H_0$, the mean is a 3-8% overestimate. The new method also has greatly reduced scatter about the mean for all the clusters in the simulated catalog compared to the isothermal method. Additionally, we show that a variation on this technique shows promise in reliably determining the 3-D radial temperature profile of the cluster gas. Our new method requires no additional observational effort compared to the traditional technique. This simple change in the analysis of the cluster data results in values of $H_0$ which are consistent with other observations.
*Subject headings:* galaxies:clusters:general–cosmology:observations–hydrodynamics–methods:numerical–cosmology:cosmic microwave background

## 1. INTRODUCTION

The hot gas in clusters of galaxies is responsible for inverse Compton scattering cosmic microwave background (CMB) photons as they travel through the intracluster medium (ICM). This results in a spectral distortion of the CMB at the location of clusters on the sky, referred to as the Sunyaev & Zeldovich (1972) effect (SZE). This distortion is characterized by a low frequency decrement, and higher frequency increment in the CMB intensity. The X-ray emission in clusters consists of thermal bremsstrahlung and line emission from the same plasma that scatters the CMB.

By combining X-ray and SZE observations of clusters of galaxies, it is possible to determine independently the angular diameter distance ($D_A$) to the cluster. This measurement has been performed for a number of galaxy clusters (see e.g., Mauskopf et al. (2000), Hughes & Birkinshaw (1998), Birkinshaw & Hughes (1994)) and the value of $H_0$ calculated is systematically low compared to other methods (Cen 1998). In addition, the range of values quoted in the literature is quite broad. While more recent measurements (e.g. Udomprasert et al. (2004), Jones et al. (2005)) calculate values consistent with $H_0$ from other methods, and methodological improvements have reduced the uncertainty somewhat (e.g. Schmidt et al. (2004)), the large scatter in calculated values for $H_0$ from observed clusters is still problematic.

Electronic address: hallman@casa.colorado.edu

Previous studies have identified several complicating factors in the current method which contribute to the bias and large scatter (Inagaki et al. 1995; Roettiger et al. 1997; Lin et al. 2003). One major source of error is the assumption of isothermality in the cluster gas. Numerical simulations have shown, and observational evidence has confirmed (Vikhlinin et al. 2005), that the gas in many clusters is not isothermal, but has a radial dependence that can be described with a universal temperature profile (Loken et al. 2002). In this *Letter*, we have examined through numerical simulations the effect of the assumption of isothermality on the calculation of the Hubble constant from SZE/X-ray observations of clusters of galaxies. We show that this assumption alone can account for the bias and large scatter of the $H_0$ estimates. We suggest a new method, which dramatically improves both the accuracy and precision of this technique, bringing the cluster value for $H_0$ into excellent agreement with results from other methods.

## 2. NUMERICAL SIMULATIONS

Our simulations use the hybrid Eulerian adaptive mesh refinement hydro/N-body code *Enzo* (O'Shea et al. (2005); http://cosmos.ucsd.edu/enzo) to evolve both the dark matter and baryonic fluid in the clusters, utilizing the piecewise parabolic method (PPM) for the hydrodynamics. With up to seven levels of refinement in high density regions, we attain spatial resolution up to $\sim 16\,h^{-1}$ kpc in the clusters. We assume a concordance $\Lambda$CDM cosmological model with the following parameters: $\Omega_{\rm b} = 0.026$, $\Omega_{\rm m} = 0.3$, $\Omega_\Lambda = 0.7$, h = 0.7, and

$\sigma_8 = 0.928$. Refinement of high density regions is performed as described in Motl et al. (2004).

We have constructed a catalog of AMR refined clusters identified in the simulation volume as described in Loken et al. (2002). The catalog of clusters used in this study includes the effects of radiative cooling, models the loss of low entropy gas to stars, adds a moderate amount of supernova feedback due to Type II supernovae in the zones where stars form, and is identified as the SFF (Star Formation with Feedback) catalog in Hallman et al. (2005). The catalog includes all clusters with total mass (baryons + dark matter) greater than $10^{14} M\odot$ out to z=2 in the simulation. This catalog includes roughly 100 such clusters at z=0, and has 20 redshift intervals of output, corresponding to a total of roughly 1500 clusters in all redshift bins combined.

## 3. CALCULATION OF $H_0$ FROM SZE/X-RAY DATA

Previous calculations of $H_0$ from clusters compare the distance scale implied by parametric models for the X-ray and SZE emission from clusters of galaxies. This analysis assumes a known function (isothermal $\beta$-model) for the gas density as a function of radius so that the integrals

$$y = \int \sigma_T n_e(r) \frac{k_b T}{m_e c^2} dl \tag{1}$$

and

$$S_X = \frac{1}{4\pi(1+z)^4} \int n_e(r) n_H(r) \Lambda(T) dl \tag{2}$$

can be solved analytically. $n_e$ and $n_H$ are the density of electrons and protons respectively, $\Lambda(T)$ is the cooling function for the gas, and $dl$ indicates the integral along the line of sight through the cluster. The isothermal $\beta$-model is

$$n_e(r) = n_{e0} \left(1 + \left(\frac{r}{r_c}\right)^2\right)^{-\frac{3\beta}{2}}. \tag{3}$$

and factoring out the common $D_A$ yields

$$y = D_A \int \sigma_T n_e \frac{k_b T}{m_e c^2} d\xi, \tag{4}$$

$$S_X = \frac{1}{4\pi(1+z)^4} D_A \int n_e n_H \Lambda(T) d\xi, \tag{5}$$

where $d\xi$ parameterizes the integrals. Solving the integrals and using the two equations to eliminate the dependence on $n_{e0}$ gives

$$D_A = \frac{{y_0}^2}{4\pi\kappa(1+z)^4 S_{x0}} \left(\frac{m_e c^2}{k_B T_e \sigma_T}\right)^2 \frac{\Lambda(T)}{\theta_c \sqrt{\pi}} F(\beta), \tag{6}$$

where $\theta_c$ is the core radius of the cluster in angular units, $\kappa = \mu_H/\mu_e$, and $F(\beta)$ is the combination of gamma functions

$$F(\beta) = \frac{\Gamma(3\beta - 0.5)}{\Gamma(3\beta)} \left(\frac{\Gamma(\frac{3}{2}\beta)}{\Gamma(\frac{3}{2}\beta - 0.5)}\right)^2 \tag{7}$$

(Lin et al. 2003).

### 3.1. *A New Method for Calculating $H_0$ from Clusters*

Previous studies suggest that the assumption of isothermality in the analysis of clusters for determination of mass, as well as the Hubble constant leads to biased estimates of both quantities (Hallman et al. 2005; Roettiger et al. 1997; Lin et al. 2003). While some of these previous studies have compared results obtained with non-isothermal $\beta$-models, we take a more general approach. We make no assumption about the density profile of the cluster, but assume that the radial temperature dependence is described by a universal temperature profile (UTP)

$$T(r) = \langle T \rangle_{500} T_0 \left(1 + \left(\frac{r}{\alpha r_{500}}\right)^2\right)^{-\delta}, \tag{8}$$

where $r_{500}$ indicates the radius associated with a mean overdensity with respect to the critical density of 500. Similarly, $T_{500}$ indicates the average spectral (in this study, emission-weighted) temperature inside $r_{500}$. $T_0$, $\alpha$, and $\delta$ are fitted parameters to the distribution of all clusters at each redshift in the simulations used in this study. The mean values of these parameters for clusters at select redshifts are shown in Table 1. We have used the redshift-specific value for each cluster in the analysis.

With surface brightness profiles from X-ray and SZE observations, we perform a geometric deprojection of these profiles under the assumption of spherical symmetry. In the deprojection case, we make no assumption about the density distribution in the cluster, therefore the integrals in Equations 4 and 5 cannot be solved *a priori*. Geometric deprojection is performed by the following calculation, as in Kriss et al. (1983)

$$\epsilon = (Vol^T)^{-1} \cdot L_{ring}, \tag{9}$$

where $L_{ring}$ is the luminosity in each annulus around the cluster center, $\epsilon$ is the emissivity in each corresponding shell with the same physical bin width as the annulus, and $Vol$ is the matrix which describes the volume in each shell which is projected into each of the annuli. The dot represents in this case the matrix product. Given an assumption of the gas temperature in each shell, it is possible to determine the three-dimensional density profile of the cluster via this method. Our value for the temperature in each shell comes from Equation 8, normalized by the average projected emission weighted temperature inside $r_{500}$. We can then calculate the density profile of the cluster from a geometric deprojection of the X-ray surface brightness, or from the SZE alone.

However, if we assume we do not know the value of $D_A$, then the values of $Vol$ are known only as functions of $D_A$ and the angular scale of each annulus. Factoring out $D_A$, we get

$$\epsilon = {D_A}^{-3} (V_\theta^T)^{-1} \cdot L_{ring}, \tag{10}$$

where $V_\theta$ indicates the volume matrix calculated in angular units. We solve for emissivity in each shell, for both the X-ray and SZE surface brightness profile. Using the UTP to set the temperature in each shell, we then extract the radial density profile as a function of $D_A$. When doing the deprojection in angular units, we have in fact calculated in each case the value of $\epsilon {D_A}^3$. Then, solving for density in each shell, we have

$$n_e^{sze}(\theta) \propto \epsilon_y {D_A}^3, \tag{11}$$

TABLE 1
Mean parameters for Universal Temperature Profile

| Parameter | $z=0$ | $z=0.1$ | $z=0.25$ | $z=0.5$ | $z=1.0$ |
|---|---|---|---|---|---|
| $T_0$ | 1.25±0.06[a] | 1.27±0.06 | 1.31±0.08 | 1.37±0.09 | 1.37±0.14 |
| $\delta$ | 0.51±0.21 | 0.51±0.19 | 0.42±0.13 | 0.43±0.12 | 0.53±0.22 |
| $\alpha$ | 1.17±0.46 | 1.12±0.40 | 0.91±0.34 | 0.80±0.28 | 0.90±0.45 |

[a]All errors are $1\sigma$.

TABLE 2
Ratio of Estimated Hubble Constant to True Value, $r_{500}$

| Method | Sample | Mean | Median | $\sigma_m$[1] | 95%upper | 95%lower |
|---|---|---|---|---|---|---|
| Isothermal | Full | 0.811 | 0.734 | 0.01 | 1.57 | 0.388 |
| Isothermal | Clean | 0.675 | 0.683 | 0.006 | 1.00 | 0.373 |
| UTP | Full | 1.08 | 1.07 | 0.0025 | 1.26 | 0.910 |
| UTP | Clean | 1.03 | 1.04 | 0.0023 | 1.13 | 0.908 |

[1]Error on the mean.

and

$$n_e^{xray}(\theta) \propto \sqrt{\epsilon_x {D_A}^3} \propto {D_A}^{\frac{3}{2}}. \quad (12)$$

Taking these values and dividing them, we calculate

$$D_{A,est} = \left( \frac{n_e^{sze}(\theta)}{n_e^{xray}(\theta)} \right)^{2/3}, \quad (13)$$

and thus the ratio

$$\frac{H_{0,est}}{H_{0,true}} \propto \frac{D_{A,true}}{D_{A,est}}. \quad (14)$$

The values of this ratio are then averaged across all radii in each cluster out to $r_{500}$.

In the cluster catalog used, the roughly 1500 clusters from z=0 to z=2 in 20 redshift bins are cut from the full simulation volume and spatially resolved projected quantities were calculated from the physical properties of the gas along each line of sight. Projections were done along each of the three principal axes on the simulation grid. These calculations include projected X-ray emissivity (surface brightness), Compton $y$-parameter, and emission-weighted temperature. Two of the three projections were selected randomly for each cluster, and radial profiles of X-ray surface brightness and Compton $y$-parameter were generated for each of the selected projected images. Also, the average projected emission-weighted temperature inside $r_{500}$ was calculated to normalize the UTP.

We have analyzed the simulated cluster observables just as would be done with clusters observed in the real universe. The simulated observations are idealized, of course, since no instrumental effects or foreground/background removal are simulated. Each of the radial profiles inside $r_{500}$ of surface brightness and Compton $y$ were fit individually to isothermal $\beta$ models, as well as geometrically deprojected. The parameters of the UTP result from a fit to the three-dimensional temperature profiles of the full cluster population at each redshift. The methods described above are then applied to determine the ratio of the estimated Hubble constant to the true value. The angular scale of the annuli in each image is calculated from the true angular diameter distance at each simulation redshift for the cosmology assumed.

## 4. RESULTS

The results of the calculation of $H_0$ via the new method described above are summarized in Table 2 and Figure 1 for clusters at all redshifts in the simulation. Figure 1 shows the histogram for values of the ratio of the estimated Hubble constant to the true value for the two methods described here. The red line is for the full sample of clusters at all redshifts using the UTP deprojection method. The green line is the distribution of values for the same set of clusters, but using the isothermal method. While the isothermal method results in a biased mean and median value, it also has a broad distribution with a long tail of overestimated values of $H_0$. The UTP method, by contrast, gives a much narrower distribution, with only a small bias in the median and mean, which has the correct value within the 95% scatter of the sample.

The black and blue lines result from cleaning of the sample as described in Hallman et al. (2005). This cleaning is done on a qualitative basis, and removes all clusters with apparently disturbed morphology, double peaks in surface brightness, or cooling cores. This cleaning of the sample removes roughly 75% of all cluster projected images from z=0 to z=2, though a large fraction of those are at redshifts greater than z=0.5. Cleaning the sample both reduces the scatter and shifts the mean and median values downward, removing the high end tail of the distribution. This is a result of pulling out many of the clusters with "boosted" surface brightness. The bias in the mean value of $H_0$ from the isothermal method still remains, and is in fact bigger than in the full sample. The UTP method has a reduced bias in the median and mean when the sample is cleaned for obviously disturbed clusters.

## 5. OTHER APPLICATIONS OF DEPROJECTION TECHNIQUES

It is important to note that if one presumes knowledge of $D_A$ and $H_0$ from other observations, one can use the combination of SZE/X-ray observations to determine the cluster density profile, and consequently the mass of the cluster (e.g., Hallman et al. (2005)). Additionally, this combination can be used to determine the three-dimensional spherically symmetric radial gas temperature profile of the cluster (e.g., Kitayama et al. (2004); Cavaliere et al. (2005)). We have done initial tests of this technique on our cluster catalog, and discovered that it is indeed possible to extract a relatively accurate value for the true gas temperature of the cluster. This method is independent of X-ray spectral temperature methods, so it can be used to determine the correct scaling between bulk spectral temperature and the normalization of a universal temperature profile. The inital test uses a method similar to that described above, but instead extracts the temperature at a radius of approximately 200 $kpc$, roughly the core radius of clusters in our mass range. We then compare that value to the true gas temperature at the same radius on the simulation grid for each cluster. The mean ratio of estimated temperature to true temperature ($T_{est}/T_{true}$) from this method for the clusters in the catalog at $z=0$ is $T_{est}/T_{true} = 0.97 \pm 0.15$ to $1\sigma$. A more thorough analysis of the accuracy of this technique is left to future work.

## 6. CONCLUSIONS

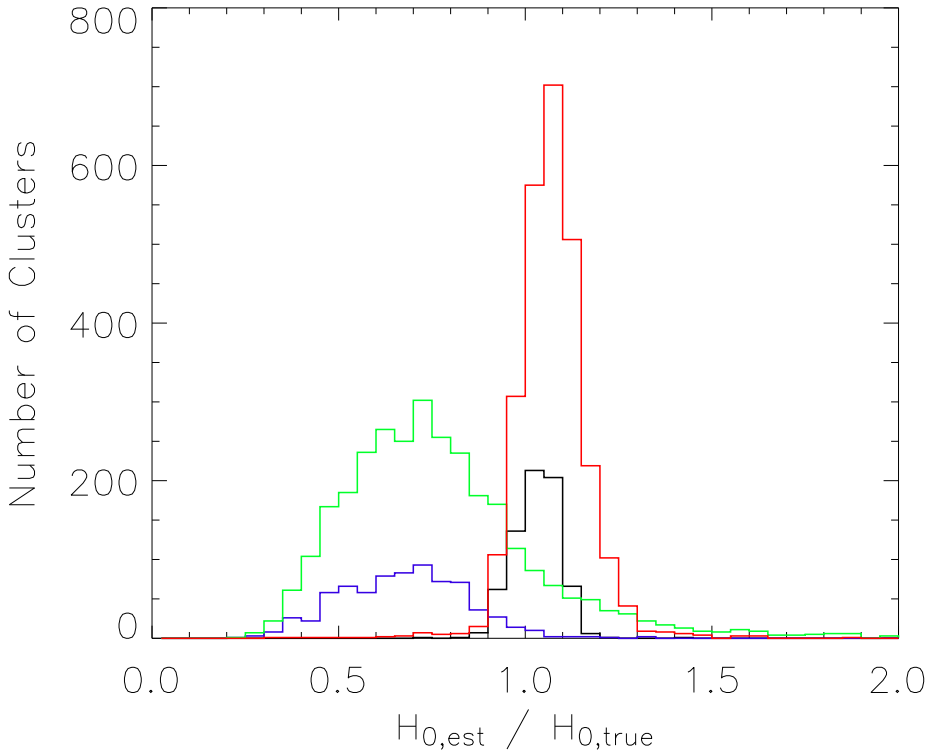


FIG. 1.— Histogram of clusters in simulated catalog ratio of estimated Hubble constant to true value. Green and blue lines indicate values from method assuming isothermality of the cluster gas, red and black lines are for geometric deprojection assuming a universal temperature profile. Red and green are for the full cluster sample, blue and black are for the sample cleaned of merging, disturbed, and cooling core clusters.

We have presented a new method for calculating $H_0$ from X-ray/SZE observations of clusters of galaxies which results in a much more precise and accurate value for $H_0$ than previous methods. This new method does not assume isothermality for the cluster gas, but assumes the gas has a radial dependence of temperature described by a universal temperature profile. The surface brightness is geometrically deprojected under the assumption of spherical symmetry. In particular, the new method does not suffer from the bias in the mean and median values which is generated by the assumption of isothermality in the calculation. Our study suggests that for a large cluster sample cleaned of obvious mergers and disturbed morphology clusters, the mean value for $H_0$ calculated assuming isothermal cluster gas will be more than a 30% underestimate of the true value. By contrast, our new method results in about an 3% overestimate in the mean value of $H_0$ for the same sample of clusters. This method also has greatly reduced scatter around the mean of the distribution than does the isothermal method. Critically important is that this technique requires no additional observational information about each cluster than does the typically used method, but only requires surface brightness profiles of X-ray and SZE, as well as an average temperature for the cluster. Additionally, X-ray/SZE deprojection methods show promise in accurately calculating both gas density and three-dimensional radial temperature profiles of the cluster gas without appealing to the assumption of hydrostatic equilbrium.

While previous studies have attempted to modify the standard method of calculating $H_0$ by using non-isothermal $\beta$-models (e.g. Lin et al. (2003)), or extending the pressure profile of the cluster under other assumptions (e.g. Schmidt et al. (2004)), we have made no direct assumption about the density profile of the cluster. The identified discrepancy between $H_0$ calculated from studies of the cosmic microwave background, or from high redshift supernovae and the value calculated from clusters is apparently largely a result of the assumption of isothermality. This new, and simple method applied to observations of galaxy clusters should correct this discrepancy.

The simulations presented in this work were conducted at the National Center for Supercomputing Applications at the University of Illinois, Urbana-Champaign through computer allocation grant AST010014N. We wish to acknowledge the support of the Chandra X-ray science center and NASA through grant TM3-4008A. We also acknowledge the support of the NSF through grant AST-0407368.

REFERENCES

Birkinshaw, M. & Hughes, J. P. 1994, ApJ, 420, 33

Cavaliere, A., Lapi, A., & Rephaeli, Y. 2005, ArXiv Astrophysics e-prints, astro-ph/0508287

Cen, R. 1998, ApJ, 498, L99+
Hallman, E. J., Motl, P. M., Burns, J. O., & Norman, M. L. 2005, ArXiv Astrophysics e-prints, astro-ph/0509460
Hughes, J. P. & Birkinshaw, M. 1998, ApJ, 501, 1
Inagaki, Y., Suginohara, T., & Suto, Y. 1995, PASJ, 47, 411
Jones, M. E., Edge, A. C., Grainge, K., Grainger, W. F., Kneissl, R., Pooley, G. G., Saunders, R., Miyoshi, S. J., Tsuruta, T., Yamashita, K., Tawara, Y., Furuzawa, A., Harada, A., & Hatsukade, I. 2005, MNRAS, 357, 518
Kitayama, T., Komatsu, E., Ota, N., Kuwabara, T., Suto, Y., Yoshikawa, K., Hattori, M., & Matsuo, H. 2004, PASJ, 56, 17
Kriss, G. A., Cioffi, D. F., & Canizares, C. R. 1983, ApJ, 272, 439
Lin, W.-C., Norman, M. L., & Bryan, G. L. 2003, ArXiv Astrophysics e-prints, astro-ph/0303355
Loken, C., Norman, M. L., Nelson, E., Burns, J., Bryan, G. L., & Motl, P. 2002, ApJ, 579, 571
Mauskopf, P. D., Ade, P. A. R., Allen, S. W., Church, S. E., Edge, A. C., Ganga, K. M., Holzapfel, W. L., Lange, A. E., Rownd, B. K., Philhour, B. J., & Runyan, M. C. 2000, ApJ, 538, 505
Motl, P. M., Burns, J. O., Loken, C., Norman, M. L., & Bryan, G. 2004, ApJ, 606, 635
O'Shea, B. W., Bryan, G., Bordner, J., Norman, M. L., Abel, T., Harkness, R., & Kritsuk, A. 2005, in Adaptive Mesh Refinement: Theory and Applications (Berlin: Springer), 341
Roettiger, K., Stone, J. M., & Mushotzky, R. F. 1997, ApJ, 482, 588
Schmidt, R. W., Allen, S. W., & Fabian, A. C. 2004, MNRAS, 352, 1413
Sunyaev, R. A. & Zeldovich, Y. B. 1972, Comments on Astrophysics and Space Physics, 4, 173
Udomprasert, P. S., Mason, B. S., Readhead, A. C. S., & Pearson, T. J. 2004, ApJ, 615, 63
Vikhlinin, A., Markevitch, M., Murray, S. S., Jones, C., Forman, W., & Van Speybroeck, L. 2005, ApJ, 628, 655